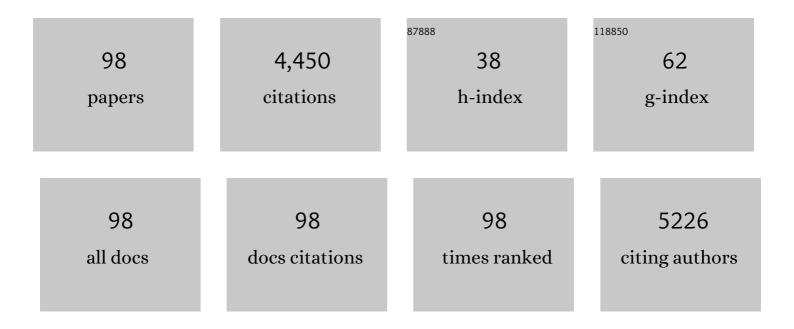
Yongfeng Li

List of Publications by Year in descending order

Source: https://exaly.com/author-pdf/7590880/publications.pdf Version: 2024-02-01



#	Article	IF	CITATIONS
1	Mesoporous, Three-Dimensional Wood Membrane Decorated with Nanoparticles for Highly Efficient Water Treatment. ACS Nano, 2017, 11, 4275-4282.	14.6	392
2	Synthesis and microwave absorption property of flexible magnetic film based on graphene oxide/carbon nanotubes and Fe ₃ O ₄ nanoparticles. Journal of Materials Chemistry A, 2014, 2, 14940.	10.3	306
3	Lightweight hollow carbon nanospheres with tunable sizes towards enhancement in microwave absorption. Carbon, 2016, 108, 234-241.	10.3	221
4	Highly active TiO2/g-C3N4/G photocatalyst with extended spectral response towards selective reduction of nitrobenzene. Applied Catalysis B: Environmental, 2017, 203, 1-8.	20.2	185
5	Enhanced Electromagnetic Microwave Absorption Property of Peapod-like MnO@carbon Nanowires. ACS Applied Materials & Interfaces, 2018, 10, 40078-40087.	8.0	126
6	Carbon nitride template-directed fabrication of nitrogen-rich porous graphene-like carbon for high performance supercapacitors. Carbon, 2018, 130, 325-332.	10.3	124
7	High graphite N content in nitrogen-doped graphene as an efficient metal-free catalyst for reduction of nitroarenes in water. Green Chemistry, 2016, 18, 4254-4262.	9.0	109
8	Phosphorus doped nickel-molybdenum aerogel for efficient overall water splitting. Applied Catalysis B: Environmental, 2021, 298, 120494.	20.2	105
9	Atomically dispersed Ni as the active site towards selective hydrogenation of nitroarenes. Green Chemistry, 2019, 21, 704-711.	9.0	98
10	Preparation of graphene nanosheets by shear-assisted supercritical CO 2 exfoliation. Chemical Engineering Journal, 2016, 284, 78-84.	12.7	91
11	Dual-template endowing N, O co-doped hierarchically porous carbon from potassium citrate with high capacitance and rate capability for supercapacitors. Chemical Engineering Journal, 2021, 417, 129289.	12.7	91
12	Magnetic coupling engineered porous dielectric carbon within ultralow filler loading toward tunable and high-performance microwave absorption. Journal of Materials Science and Technology, 2021, 70, 214-223.	10.7	74
13	Dielectric composite reinforced by in-situ growth of carbon nanotubes on boron nitride nanosheets with high thermal conductivity and mechanical strength. Chemical Engineering Journal, 2019, 358, 718-724.	12.7	73
14	P-doped nanomesh graphene with high-surface-area as an efficient metal-free catalyst for aerobic oxidative coupling of amines. Carbon, 2017, 121, 443-451.	10.3	69
15	Sulfur-doped porous carbon as metal-free counter electrode for high-efficiency dye-sensitized solar cells. Journal of Power Sources, 2015, 282, 228-234.	7.8	67
16	Intrinsic defect-rich porous carbon nanosheets synthesized from potassium citrate toward advanced supercapacitors and microwave absorption. Carbon, 2021, 183, 176-186.	10.3	67
17	Three-dimensional skeleton assembled by carbon nanotubes/boron nitride as filler in epoxy for thermal management materials with high thermal conductivity and electrical insulation. Composites Part B: Engineering, 2021, 224, 109168.	12.0	66
18	Production of hierarchical porous carbon nanosheets from cheap petroleum asphalt toward lightweight and high-performance electromagnetic wave absorbents. Carbon, 2020, 166, 218-226.	10.3	63

#	Article	IF	CITATIONS
19	Enhanced Electromagnetic Microwave Absorption Performance of Lightweight Bowl-like Carbon Nanoparticles. Industrial & Engineering Chemistry Research, 2017, 56, 11460-11466.	3.7	61
20	Synthesis of graphene/α-Fe ₂ O ₃ composites with excellent electromagnetic wave absorption properties. RSC Advances, 2015, 5, 60114-60120.	3.6	60
21	Glycine functionalized boron nitride nanosheets with improved dispersibility and enhanced interaction with matrix for thermal composites. Chemical Engineering Journal, 2021, 408, 127360.	12.7	57
22	Heteroatoms-doped hierarchical porous carbon with multi-scale structure derived from petroleum asphalt for high-performance supercapacitors. Carbon, 2022, 187, 338-348.	10.3	57
23	Controllable and eco-friendly synthesis of P-riched carbon quantum dots and its application for copper (II) ion sensing. Applied Surface Science, 2018, 448, 589-598.	6.1	55
24	High-surface-area nanomesh graphene with enriched edge sites as efficient metal-free cathodes for dye-sensitized solar cells. Nanoscale, 2016, 8, 13059-13066.	5.6	53
25	Construction of efficient counter electrodes for dye-sensitized solar cells: Fe2O3 nanoparticles anchored onto graphene frameworks. Carbon, 2016, 96, 947-954.	10.3	53
26	Reduced graphene oxide supported Pd-Cu-Co trimetallic catalyst: synthesis, characterization and methanol electrooxidation properties. Journal of Energy Chemistry, 2019, 29, 72-78.	12.9	53
27	Highly active and reflective MoS2 counter electrode for enhancement of photovoltaic efficiency of dye sensitized solar cells. Electrochimica Acta, 2016, 212, 614-620.	5.2	50
28	Ultralow concentration of molybdenum disulfide nanosheets for enhanced oil recovery. Fuel, 2019, 251, 514-522.	6.4	50
29	Insight into the topological defects and dopants in metal-free holey graphene for triiodide reduction in dye-sensitized solar cells. Journal of Materials Chemistry A, 2017, 5, 5952-5960.	10.3	49
30	Fabrication of porous graphene-like carbon nanosheets with rich doped-nitrogen for high-performance electromagnetic microwave absorption. Applied Surface Science, 2020, 530, 147298.	6.1	49
31	Shear-Assisted Production of Few-Layer Boron Nitride Nanosheets by Supercritical CO2 Exfoliation and Its Use for Thermally Conductive Epoxy Composites. Scientific Reports, 2017, 7, 17794.	3.3	46
32	Phosphorus-doped porous graphene nanosheet as metal-free electrocatalyst for triiodide reduction reaction in dye-sensitized solar cell. Applied Surface Science, 2017, 405, 308-315.	6.1	45
33	In-situ activation endows the integrated Fe3C/Fe@nitrogen-doped carbon hybrids with enhanced pseudocapacitance for electrochemical energy storage. Chemical Engineering Journal, 2019, 375, 122061.	12.7	45
34	Plasma synthesis of carbon nanotube-gold nanohybrids: efficient catalysts for green oxidation of silanes in water. Journal of Materials Chemistry A, 2014, 2, 245-250.	10.3	44
35	Synthesis of three-dimensional graphene from petroleum asphalt by chemical vapor deposition. Materials Letters, 2014, 122, 285-288.	2.6	43
36	Transverse size effect on electromagnetic wave absorption performance of exfoliated thin-layered flake graphite. Carbon, 2019, 153, 682-690.	10.3	40

#	Article	IF	CITATIONS
37	Self-reconstruction strategy to synthesis of Ni/Co-OOH nanoflowers decorated with N, S co-doped carbon for high-performance energy storage. Chemical Engineering Journal, 2020, 396, 125323.	12.7	40
38	Silica nanosphere supported palladium nanoparticles encapsulated with graphene: High-performance electrocatalysts for methanol oxidation reaction. Applied Surface Science, 2018, 452, 11-18.	6.1	39
39	In-situ formation of oxygen-vacancy-rich NiCo2O4/nitrogen-deficient graphitic carbon nitride hybrids for high-performance supercapacitors. Electrochimica Acta, 2020, 340, 135996.	5.2	39
40	Hierarchical MoP Hollow Nanospheres Anchored on a N,P,Sâ€Doped Porous Carbon Matrix as Efficient Electrocatalysts for the Hydrogen Evolution Reaction. ChemSusChem, 2019, 12, 4662-4670.	6.8	38
41	N, S Codoped Hierarchical Porous Graphene Nanosheets Derived from Petroleum Asphalt via in Situ Texturing Strategy for High-Performance Supercapacitors. Industrial & Engineering Chemistry Research, 2019, 58, 4487-4494.	3.7	37
42	Au/graphene oxide/carbon nanotube flexible catalyst film: synthesis, characterization and its application for catalytic reduction of 4-nitrophenol. RSC Advances, 2015, 5, 37710-37715.	3.6	34
43	Probing the charging and discharging behavior of K-CO2 nanobatteries in an aberration corrected environmental transmission electron microscope. Nano Energy, 2018, 53, 544-549.	16.0	34
44	Fabrication of ternary NaTaO3/g-C3N4/G heterojunction photocatalyst with enhanced activity for Rhodamine B degradation. Journal of Alloys and Compounds, 2019, 805, 802-810.	5.5	34
45	RGO-wrapped Ti3C2/TiO2 nanowires as a highly efficient photocatalyst for simultaneous reduction of Cr(VI) and degradation of RhB under visible light irradiation. Journal of Alloys and Compounds, 2021, 874, 159865.	5.5	33
46	Cold-adapted bacteria for bioremediation of crude oil-contaminated soil. Journal of Chemical Technology and Biotechnology, 2016, 91, 2286-2297.	3.2	31
47	Flexible and densified graphene/waterborne polyurethane composite film with thermal conducting property for high performance electromagnetic interference shielding. Nano Research, 2022, 15, 9926-9935.	10.4	30
48	Controllable synthesis of single- and double-walled carbon nanotubes from petroleum coke and their application to solar cells. Carbon, 2014, 68, 511-519.	10.3	29
49	Assembling Graphene-Encapsulated Pd/TiO2 Nanosphere with Hierarchical Architecture for High-Performance Visible-Light-Assisted Methanol Electro-Oxidation Material. Industrial & Engineering Chemistry Research, 2019, 58, 19486-19494.	3.7	29
50	Supercritical fluid extraction with carbon nanotubes as a solid collection trap for the analysis of polycyclic aromatic hydrocarbons and their derivatives. Journal of Chromatography A, 2015, 1395, 1-6.	3.7	28
51	S-Doped Porous Graphene Microspheres with Individual Robust Red-Blood-Cell-Like Microarchitecture for Capacitive Energy Storage. Industrial & Engineering Chemistry Research, 2017, 56, 9524-9532.	3.7	27
52	Construction of Graphene-Wrapped Pd/TiO ₂ Hollow Spheres with Enhanced Anti-CO Poisoning Capability toward Photoassisted Methanol Oxidation Reaction. ACS Sustainable Chemistry and Engineering, 2021, 9, 1352-1360.	6.7	27
53	Scalable Production of Hydrophilic Graphene Nanosheets via in Situ Ball-Milling-Assisted Supercritical CO ₂ Exfoliation. Industrial & Engineering Chemistry Research, 2017, 56, 6939-6944.	3.7	26
54	Synthesis of Sandwich-Like Nanostructure Fillers and Their Use in Different Types of Thermal Composites. ACS Applied Materials & Interfaces, 2019, 11, 40694-40703.	8.0	26

#	Article	IF	CITATIONS
55	Facile fabrication of Fe/Fe5C2@N-doped porous carbon as an efficient microwave absorbent with strong and broadband absorption properties at an ultralow filler loading. Carbon, 2022, 196, 890-901.	10.3	26
56	Green production of hydrogen by hydrolysis of graphene-modified aluminum through infrared light irradiation. Chemical Engineering Journal, 2017, 320, 160-167.	12.7	25
57	Atomic N-coordinated cobalt sites within nanomesh graphene as highly efficient electrocatalysts for triiodide reduction in dye-sensitized solar cells. Chemical Engineering Journal, 2018, 349, 782-790.	12.7	24
58	Preparation of an efficient Fe/N/C electrocatalyst and its application for oxygen reduction reaction in alkaline media. Journal of Electroanalytical Chemistry, 2018, 810, 62-68.	3.8	23
59	In Situ-Generated Volatile Precursor for CVD Growth of a Semimetallic 2D Dichalcogenide. ACS Applied Materials & Interfaces, 2018, 10, 34401-34408.	8.0	23
60	Density Functional Theory Study of the Formaldehyde Catalytic Oxidation Mechanism on a Au-Doped CeO2(111) Surface. Journal of Physical Chemistry C, 2018, 122, 438-448.	3.1	22
61	Crumpled Nitrogen-Doped Porous Carbon Nanosheets Derived from Petroleum Pitch for High-Performance and Flexible Electromagnetic Wave Absorption. Industrial & Engineering Chemistry Research, 2022, 61, 2799-2808.	3.7	22
62	Silicon doped graphene as high cycle performance anode for lithium-ion batteries. Carbon, 2022, 196, 633-638.	10.3	22
63	Controllable synthesis of single-, double- and triple-walled carbon nanotubes from asphalt. Chemical Engineering Journal, 2013, 225, 210-215.	12.7	21
64	Interconnected nitrogen and sulfur dual-doped porous carbon as efficient electrocatalyst for triiodide reduction in dye-sensitized solar cells. Journal of Power Sources, 2016, 327, 289-296.	7.8	21
65	Cobalt single atoms anchored on nitrogen-doped porous carbon as an efficient catalyst for oxidation of silanes. Green Chemistry, 2021, 23, 1026-1035.	9.0	21
66	Electrochemical activation induced phase and structure reconstruction to reveal cobalt sulfide intrinsic energy storage capacity. Chemical Engineering Journal, 2022, 434, 134473.	12.7	21
67	High-Efficiency Production of Graphene by Supercritical CO ₂ Exfoliation with Rapid Expansion. Langmuir, 2018, 34, 7797-7804.	3.5	20
68	The fabrication of Cu nanowire/graphene/Al doped ZnO transparent conductive film on PET substrate with high flexibility and air stability. Materials Letters, 2017, 207, 62-65.	2.6	19
69	Crumpled graphene prepared by a simple ultrasonic pyrolysis method for fast photodetection. Carbon, 2018, 128, 117-124.	10.3	19
70	Synergistic effects of nitrogen-doped graphene and Fe2O3 nanocomposites in catalytic oxidization of aldehyde with O2. Chemical Engineering Journal, 2017, 330, 880-889.	12.7	18
71	Enhanced electromagnetic wave absorption of worm-like hollow porous MnO@C/CNTs composites. Journal of Alloys and Compounds, 2019, 797, 1086-1094.	5.5	18
72	Sulfur-fixation strategy toward controllable synthesis of molybdenum-based/carbon nanosheets derived from petroleum asphalt. Chemical Engineering Journal, 2020, 380, 122552.	12.7	18

#	Article	IF	CITATIONS
73	Highly Efficient Water Splitting Catalyst Composed of N,P-Doped Porous Carbon Decorated with Surface P-Enriched Ni ₂ P Nanoparticles. ACS Applied Materials & Interfaces, 2022, 14, 20358-20367.	8.0	18
74	Facile Synthesis of Well-Dispersed Ni2P on N-Doped Nanomesh Carbon Matrix as a High-Efficiency Electrocatalyst for Alkaline Hydrogen Evolution Reaction. Nanomaterials, 2019, 9, 1022.	4.1	16
75	Construction of MnO-skeleton cross-linked by carbon nanotubes networks for efficient microwave absorption. Journal of Colloid and Interface Science, 2021, 602, 778-788.	9.4	16
76	Scalable production of few-layer molybdenum disulfide nanosheets by supercritical carbon dioxide. Journal of Materials Science, 2018, 53, 7258-7265.	3.7	15
77	Nitrogen-Enriched Hollow Carbon Spheres Coupled with Efficient Co–Nx–C Species as Cathode Catalysts for Triiodide Reduction in Dye-Sensitized Solar Cells. ACS Sustainable Chemistry and Engineering, 2019, 7, 2679-2685.	6.7	15
78	Enhanced thermal conductivity and isotropy of polymer composites by fabricating <scp>3D</scp> network structure from carbonâ€based materials. Journal of Applied Polymer Science, 2021, 138, 49781.	2.6	15
79	Water-soluble salt-templated strategy to regulate mesoporous nanosheets-on-network structure with active mixed-phase CoO/Co3O4 nanosheets on graphene for superior lithium storage. Journal of Alloys and Compounds, 2021, 857, 157626.	5.5	15
80	Sulfur-doped porous graphene frameworks as an efficient metal-free electrocatalyst for oxygen reduction reaction. Materials Letters, 2018, 214, 209-212.	2.6	14
81	Organochlorine Compounds with a Low Boiling Point in Desalted Crude Oil: Identification and Conversion. Energy & amp; Fuels, 2018, 32, 6475-6481.	5.1	13
82	Synthesis of Ultralight N-Rich Porous Graphene Nanosheets Derived from Fluid Catalytic Cracking Slurry and Their Electromagnetic Wave Absorption Properties. Industrial & Engineering Chemistry Research, 2020, 59, 8243-8251.	3.7	13
83	In-situ bonding with sulfur in petroleum asphalt to synthesize transition metal (Mn, Mo, Fe, or) Tj ETQq1 1 0.78	84314 rgBT 10.9	/Oygrlock 10
84	Exfoliated multi-layered graphene anode with the broadened delithiation voltage plateau below 0.5ÂV. Journal of Energy Chemistry, 2020, 49, 233-242.	12.9	12
85	Synergistic effect of size distribution on the electrical and thermal conductivities of graphene-based paper. Journal of Materials Science, 2018, 53, 10261-10269.	3.7	11
86	Enhanced catalytic hydrogen evolution reaction performance of highly dispersed Ni2P nanoparticles supported by P-doped porous carbon. Colloids and Surfaces A: Physicochemical and Engineering Aspects, 2021, 616, 126308.	4.7	10
87	Electrochemical synthesis of FeNx doped carbon quantum dots for sensitiveÂdetection of Cu2+ ion. Green Energy and Environment, 2023, 8, 141-150.	8.7	9
88	Construction of a Graphene-Wrapped Pd/SiO ₂ @TiO ₂ Core–Shell Sphere for Enhanced Photoassisted Electrocatalytic Methanol Oxidation Property. Industrial & Engineering Chemistry Research, 2020, 59, 13380-13387.	3.7	8
89	Tuning surface chemical property in hierarchical porous carbon via nitrogen and phosphorus doping for deep desulfurization. Separation and Purification Technology, 2022, 280, 119923.	7.9	7
90	Theoretical study of structure sensitivity on Au doped CeO2 surfaces for formaldehyde oxidation: The effect of crystal planes and Au doping. Chemical Engineering Journal, 2022, 433, 133599.	12.7	7

#	Article	IF	CITATIONS
91	Electronic structure regulation of CoMoS catalysts by N, P co-doped carbon modification for effective hydrodesulfurization. Fuel, 2022, 322, 124160.	6.4	7
92	C59N Peapods Sensing the Temperature. Sensors, 2013, 13, 966-974.	3.8	5
93	In-situ observation of electrochemically driven Kirkendall effect induced volume shrinkage of CuO nanowires during potassiation. Materials Letters, 2019, 237, 340-343.	2.6	3
94	Scalable preparation of water-soluble ink of few-layered WSe ₂ nanosheets for large-area electronics*. Chinese Physics B, 2020, 29, 066802.	1.4	3
95	Finding a Cheaper Carbon Source: High-Quality, Single-Walled Nanotubes from Asphalt and Petroleum Coke. IEEE Nanotechnology Magazine, 2013, 7, 15-18.	1.3	2
96	Nitrogen and Phosphorus Coâ€Doped Grapheneâ€Like Carbon Catalyzed Selective Oxidation of Alcohols. Asian Journal of Organic Chemistry, 2019, 8, 422-427.	2.7	2
97	High-quality single-walled carbon nanotubes synthesized from asphalt and petroleum coke. , 2013, , .		Ο
98	Green production of silica hydroxyl riched palygorskite by shear-assisted supercritical CO2 separation process for dye adsorption and heavy oil viscosity reduction. Applied Clay Science, 2021, 212, 106207.	5.2	0